Spectral analysis of 24 GRBs/XRFs observed with HETE-2/FREGATE

C. Barraud,[1] J-F. Olive,[2] J.P. Lestrade,[1,⋆] J-L. Atteia,[1] K. Hurley,[3] G. Ricker,[4] D. Q. Lamb,[5] N. Kawai,[6,7] M. Boer,[2] J-P. Dezalay,[2] G. Pizzichini,[12] R. Vanderspek,[4] G. Crew,[4] J. Doty,[4] G. Monelly,[4] J. Villasenor,[4] N. Butler,[4] A. Levine,[4] A. Yoshida,[6,8] Y. Shirasaki,[6,10] T. Sakamoto,[6,7,11] T. Tamagawa,[7] K. Torii,[7] M. Matsuoka,[9] E. E. Fenimore,[11] M. Galassi,[11] T. Tavenner,[11] T. Q. Donaghy[5] C. Graziani[5] and J.G. Jernigan[3]

[1] Laboratoire d'Astrophysique, Observatoire Midi-Pyrenes, 31400 Toulouse, France e-mail: barraud@ast.obs-mip.fr
[2] C.E.S.R., Observatoire Midi-Pyrenes, 31028 Toulouse Cedex, France
[3] Space Sciences Laboratory, UC Berkeley, Berkeley CA, USA
[4] Center for Space Reserach, MIT, Cambridge, MA , USA
[5] Department of Astronomy and Astrophysics, University of Chicago, 5640 South Ellis Avenue, Chicago, IL 60637, USA
[6] Department of Physics, Tokyo Institute of Technology, 2-12-1 Ookayama, Meguro-ku, Tokyo 152-8551, Japan.
[7] RIKEN, The Institute of Physical and Chemical Research, 2-1 Hirosawa, Wako, Saitama 351-0198, Japan
[8] Department of Physics, Aoyama Gakuin University, Chitosedai 6-16-1 Setagaya-ku, Tokyo 157-8572, Japan
[9] Tsukuba Space Center, National Space Development Agency of Japan, Tsukuba, Ibaraki, 305-8505, Japan
[10] National Astronomical Observatory, Osawa 2-21-1, Mitaka, Tokyo 181-8588 Japan
[11] Los Alamos National Laboratory, P.O. Box 1663, Los Alamos, NM, 87545
[12] Consiglio Nazionale delle Ricerche (IASF), via Piero Gobetti, 101-40129 Bologna, Italy

Received ; accepted

Abstract. We present a spectral analysis of 24 GRBs detected with the HETE gamma-ray detectors (the FREGATE instrument) in the energy range 6-400 keV. We measure the spectral parameters of the time integrated spectra, and present the distribution of their low energy spectral index and of their peak energy. We discuss the existence and nature of the recently discovered X-Ray Flashes and their relationship with classical GRBs.

Key words. gamma-rays: bursts

1. Introduction

The radiation mechanisms at work during the prompt phase of GRBs remain poorly understood, despite the observation of hundreds of GRB spectra and extensive theoretical work (e.g. Cohen et al. 1997, Daigne & Mochkovitch 1998, Lloyd & Petrosian 2000, Mészáros & Rees 2000, Panaitescu & Mészáros 2000, Piran 2000, Zhang & Mészáros 2002). One of the reasons for this situation is the lack of broad-band coverage of this brief phase of GRB emission (contrarily to the afterglows which can be observed from hours to days after the burst). In the recent years, however, several instruments have extended the spectral coverage of the prompt GRB emission to the X-ray range, and in the case of GRB990123, to optical wavelengths, raising hope for a better understanding of this crucial phase of GRB emission.

We present here the broad-band spectra of 24 GRBs observed by HETE/FREGATE in the energy range 6-400 keV. We analyse the time integrated spectra in order to derive the distribution of their peak energies and of their low-energy spectral indices. We also discuss the existence of a possible new class of soft bursts, called X-ray flashes.

HETE's unique instrument suite provides broad-band energy coverage of the prompt emission extending into the X-ray range. The three instruments include a gamma-ray spectrometer sensitive in the range 6-400 keV (FREGATE, Atteia et al. 2002), a Wide Field X-ray Monitor sensitive in the range 2-25 keV

Send offprint requests to: C. Barraud
⋆ On leave from Mississippi State University

(WXM, Kawai et al. 2002) and a CCD based Soft X-ray Camera working in the range 1-14 keV (SXC, Villasenor et al. 2002). In this paper we restrict our analysis to FREGATE data because this instrument, with its larger field of view, detects about two times more GRBs than WXM (HWZM=70° for FREGATE compared to 40° for the WXM) and because in most cases FREGATE data is sufficient to determine the GRB spectral parameters. We finally note that FREGATE offers for the first time a continuous coverage from a few keV to a few hundred keV *with a single instrument*. This eliminates any possible problems caused by normalizing the responses of different instruments to one another. This specificity of FREGATE appears essential when we try to understand whether events seen at low energies are of the same nature as classical GRBs seen at higher energies.

This work follows many previous studies which contributed to our understanding of the GRB spectral properties at gamma-ray energies (Band et al. 1993, Preece et al. 1998) and in hard X-rays (Strohmayer et al. 1998, Frontera et al. 2000). This paper is the first of a series devoted to the spectral analysis of the GRBs detected with HETE-2. Forthcoming papers will discuss the spectral *evolution* of bright GRBs and the broad-band spectral distribution by combining the data from FREGATE and the WXM for the events which are detected by both instruments.

2. Spectral analysis

The FREGATE instrument on board HETE-2 has three main goals: detecting GRBs and alerting the other instruments to their occurence, performing the spectroscopy of the prompt emission in hard X-rays, and monitoring the activity of hard X-ray transient sources. A detailed description of the instrument can be found in Atteia et al. (2002). FREGATE has been designed to provide reliable spectral data on the gamma-ray bursts. The detectors use cleaved NaI crystals encapsulated in a beryllium housing offering a good sensitivity at low energies (the transmission of the window is greater than 65% at 6 keV). A graded shield made of lead, tantalum, tin, copper and aluminum reduces the background and eliminates many GRBs arriving more than 70° off-axis. Two on-board sources of Baryum 133 provide a continuous monitoring of the gain of the 4 detectors (the gain control is done on the ground; there is no automatic gain control). The whole instrument has been carefully simulated with the GEANT software from the CERN (see http://wwwinfo.cern.ch/asd/geant/index.html) and the output of the simulation program has been checked and validated against extensive calibrations done with radioactive sources (9 sources, 11 energies at 5 angles). Finally the in-flight spectral response has been checked with the Crab nebula as described in Olive et al. (2002).

Figure 1 displays the angular response of FREGATE. This figure emphasizes the importance of knowing the GRB off-axis angle to perform a reliable spectral analysis. Our spectral analysis includes the following steps:

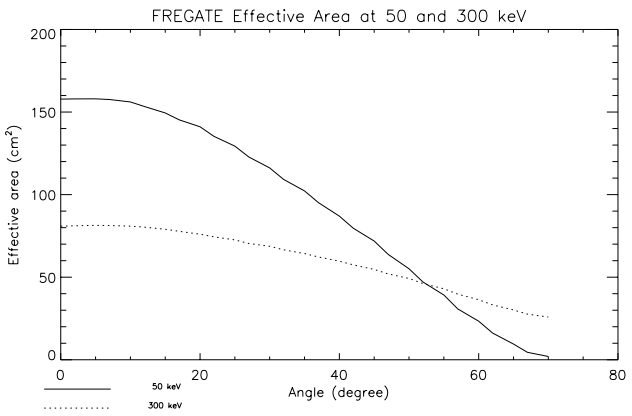

Fig. 1. FREGATE effective area as a function of the burst angle at 50 keV and 300 keV.

1. Selection of the burst sample (section 2.1).
2. Construction of gain corrected spectra and addition of the spectra from the 4 detectors.
3. Determination of the maximum energy E_{max} at which there is still some signal from the burst (Sect. 2.2).
4. Spectral deconvolution with XSPEC and determination of the spectral parameters.

2.1. The GRB sample

From October 2000 to the end of March 2002, FREGATE detected 54 confirmed GRBs of which 43 were within the 70° field of view (FOV) of the detector.[1] However not all these 43 bursts were localized and since we cannot perform accurate spectral studies of GRBs with unknown off-axis angles, we concentrate here on the analysis of the spectrum of 24 GRBs which have been localized within 60° of the detector's axis. This limiting angle ensures that we have some efficiency at low energies ($\geq$ 10%) and that the instrument response is well known. The list of these 24 GRBs is given in Table 1 with their off-axis angle and their duration T_{90}.

We should mention at this point that our sample includes one possible short/hard burst: GRB020113. In general FREGATE observes a small proportion of short/hard GRBs, with only 2 out of the 43 confirmed GRBs within the FOV of FREGATE being possible short/hard GRBs (this includes GRB020113). We presently have no explanation for this small proportion. we note however that

[1] FREGATE continuously records the count rates in 4 energy ranges ([6-40], [6-80], [32-400], and [>400] keV, see Atteia et al. 2002). GRBs outside the FOV have almost no counts below 80 keV, providing a reliable way to recognize the GRBs which are within the FOV of FREGATE, even in the absence of a localization.

FREGATE observed 2 short/hard GRBs in may 2002 (Lamb et al. 2002), raising the percentage of short hard bursts to 10% . In any case, because there is only one possible event of this type in our sample, we did not remove it.

2.2. spectral fitting

GRB spectra can in general be fit by the Band function (Band et al. 1993); that is two power laws which are smoothly connected. The photon spectrum of GRBs is thus described as follows:

$$N(E) = AE^{\alpha} \exp^{\frac{-E}{E_0}} \qquad \text{for} \quad E \leq (\alpha - \beta)E_0, \qquad \text{and}$$

$$N(E) = BE^{\beta} \qquad \text{for} \quad E \geq (\alpha - \beta)E_0, \qquad (1)$$

$$\text{where} \quad B = A[(\alpha - \beta) \times E_0]^{(\alpha - \beta)} \times \exp(\beta - \alpha).$$

Here α is the spectral index of the low energy power law, β is the spectral index of the high energy power law, and E_0 is the break energy. With this parametrization, the peak energy of the νf_ν spectrum is $E_p = E_0 \times (2+\alpha)$. E_p is well defined for $\alpha \geq -2$ and $\beta < -2$.

The first step of our processing was the definition of the spectral range appropriate for the fitting procedure. On the low energy side the limit is set to 7 keV for instrumental reasons (the electronics threshold is not well modeled below 7 keV). On the high energy side, we searched for the energy E_{max} such that the signal in the range [E_{max} - 400] keV was only two sigmas above background. The spectral fit is performed in the range [7 - E_{max}] keV, E_{max} is given in Table 1.

Most of the time this energy range is not broad enough to allow the unambiguous determination of the 4 parameters of the Band function. Consequently, we decided to fit the observed spectra using only the low energy part of the Band function and the spectral break. The definition of E_p is not affected by the choice of this model. In the following, this model is called the cutoff power law model,

$$N(E) = AE^{\alpha} \exp^{\frac{-E}{E_0}} .$$

The spectral deconvolution is done with XSPEC, using gain corrected spectra (allowing us to add up the 4 detectors) and response matrices constructed from a detailed Monte Carlo simulation of the instrument (Olive et al. 2002). The parameters resulting from the fit and their errors are given in Table 1. The cutoff power law model provides a good fit to our data as seen by reduced χ^2 values close to unity. The fit procedure takes only into account the statistical errors: no systematic errors have been added. Examples of spectral fits are given in Fig. 2.

It can be noted that the cutoff energy E_0 is well constrained for only 12 GRBs (out of 24). These events are identified in Table 1 by their name in boldface. In the following we call these GRBs group A, and group B the 12 GRBs whose E_0 is not well constrained. The fluences of group B bursts show that they are mostly faint bursts, with not enough counts at high energies to constrain E_0. It could be tempting to fit the spectra of group B bursts with a simple power law (since we have no constraint on the cutoff energy) which would give stronger constraints on α. It is not a good idea, however, to use a different model for one part of the sample because this introduces a bias in the measured values of the spectral parameters (see also Band et al. 1993). We thus keep the cutoff power law model, even when we have no constraint on E_0, and indicate in Table 1 the best fit parameters and their errors for this model. We now discuss the distribution of the spectral parameters obtained with this procedure.

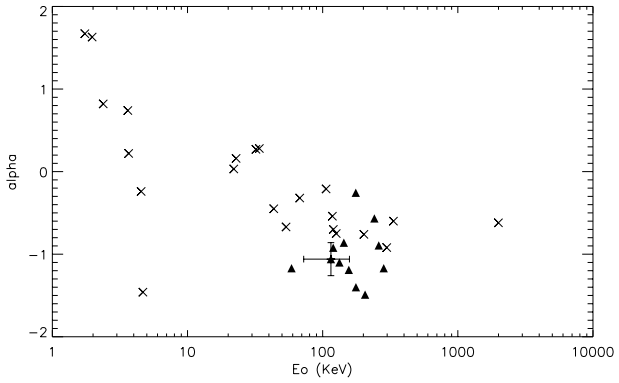

Fig. 3. Spectral parameters of 22 GRBs detected by GINGA (Strohmayer et al. 1998) and 12 GRBs detected by FREGATE. The crosses represent the GINGA points, and dark triangles the FREGATE GRBs. A typical error bar (on α and E_0) is also shown.

3. Discussion

3.1. The distribution of E_0 and α

Figure 3 displays α as a function of the cutoff energy E_0 for the events of group A. The values found in this study are superimposed on the GINGA sample published by Strohmayer et al. (1998).

To compare the GINGA and FREGATE samples we should keep in mind that the two studies differ in several ways: the GINGA fits included data from the Proportional Counter down to 2 keV while FREGATE low energy threshold is around 6 keV; the GRBs in our study arrive at known off-axis angles, while an average angle was used in the GINGA study; and finally in the Strohmayer et al. (1998) study the spectral fits were done with the Band model, while we use a cutoff power law. Using a few bright bursts which have enough statistics to be fit by a Band model, we checked that the Band model gives slightly higher values of α than the cutoff power law model. When we consider these differences between the two studies, and the size of the error bars, we conclude that the study of Strohmayer et al. (1998) and this one give similar results.

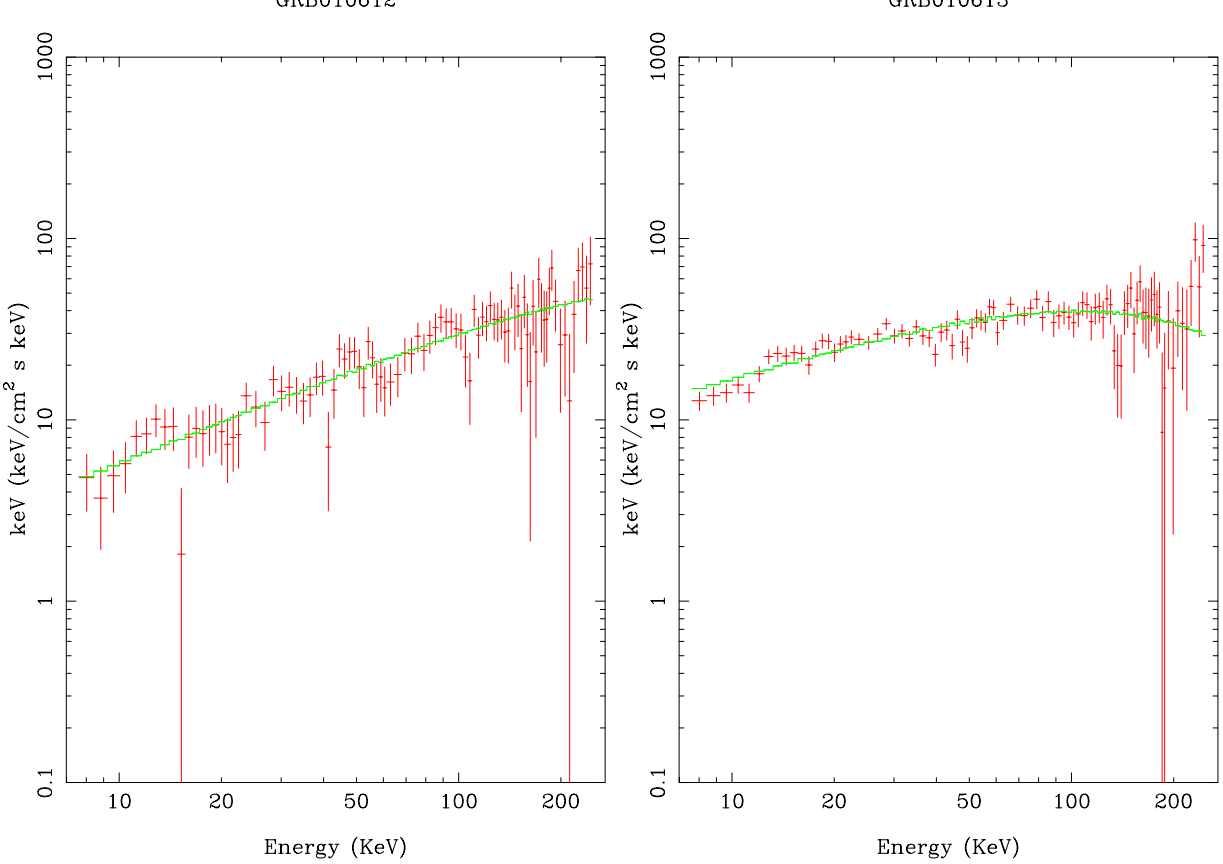

Fig. 2. Spectral fits of GRB010612 and GRB010613 with a power law with a cut-off at 600 keV and 176 keV respectively.

We note, however, a lack of events with E_0 below 50 keV in our sample, compared to the GINGA sample. As explained in section 3.1.2 below, we do not attribute this observation to a real deficit but rather to the difficulty that FREGATE has to determine E_0 for GRBs which have E_0 below a few ten keV (i.e. GRBs with few counts at high energies).

3.1.1. The distribution of α

Table 1 and Fig. 4 show that, with the exception of GRB010213 ($\alpha = -2.14$, but see discussion below), GRB010928 ($\alpha = -.567$), and GRB020214 ($\alpha = -.256$), the GRBs in our sample have α in the range $-3/2$ to $-2/3$, compatible with the values expected from radiation produced by synchrotron emission from accelerated electrons (Cohen et al. 1997, Lloyd & Petrosian 2000).

GRB010213 has the softest spectrum of our sample; its steep spectral index and high L_x/L_γ ratio are fully compatible with a GRB having a very low E_p, in any case below 20 keV. We consider that the spectral index which is measured by FREGATE is probably NOT α, but rather β. GRB010928 and GRB020214 have very hard spectra, which are definitely not compatible with synchrotron radiation in its simple form (Lloyd 2002). We fit the spectra of these 2 GRBs with the Band function, in order to check how the fit by a power law with a cutoff affected the value of α. Because these two GRBs have many high energy photons, we were able to determine the 4 parameters of the Band function. For GRB010928 we find $\alpha = -0.414$, $E_0 = 138$ keV and $\beta = -1.35$ (with the errors [-0.53;-0.28], [102;192], [-1.53;-1.26]). For GRB020214 we find $\alpha = -0.14$, $E_0 = 140$ keV and $\beta = -2.11$ (with the errors [-0.42;+0.12], [104;213], [-10;-1.75]). The fit with the Band model tends to increase the value of α, and therefore the difference with the canonical synchrotron values.

3.1.2. X-ray rich GRBs

The evidence for GRBs with low values of E_p has been accumulating over the recent years. In 1998, Strohmayer et al. (1998) studied the X-ray to γ-ray spectra of 22 GRBs (they performed joint fits of the data recorded by a proportional counter and a scintillator spanning energies from 2 to 400 keV). They found 7 GRBs with E_p lower than 10 keV and 5 more with E_p lower than 50 keV, providing the first evidence for a population of soft GRBs. In the 1990's several authors studied the distribution of E_p for BATSE GRBs (Mallozzi et al. 1995, Lloyd & Petrosian 1999, Brainerd et al. 2001). They reached the conclusion that E_p peaks around 200 keV with few GRBs having E_p below 50 keV. The situation is not so clear for high values of E_p (around 1 MeV), since BATSE could have missed a large fraction of GRBs peak-

Table 1. GRB list. This table gives the best fit parameters, the reduced χ^2 of the fit and the error bars on the spectral parameters. The names in bold indicate the events of group A (see text).

Name	Time SOD	Duration sec	Angle deg.	Loc.[a]	E_{max} keV	Chi^2(DOF)	−Alpha	errors	E_0 keV	errors	E_p	Fluence[b] $6-30$	Fluence[b] $30-400$	L_x
001225	25759	32.3	37	I	400	3.33 (104)	1.17	[1.16; 1.18]	283	$[271-296]$	235	200	1140	.1
010126	33047	7.7	50	I	220	1.12 (84)	1.06	[0.82; 1.26]	115	$[72-218]$	108	8.1	30	.2
010213	45332	20.9	14	W	200	1.11 (81)	2.14	[1.83; 2.55]	10000	$[370-1e4]$	< 20	2.0	2.4	.8
010225	60733	7.2	23	W	400	1.16 (104)	.89	$[-1.8; 2.14]$	22	$[5-1e4]$	24	1.2	0.7	1.
010326A	11701	23.0	60	I	400	0.67 (104)	.894	[0.66; 1.09]	260	$[167-484]$	287	16	160	.1
010326*B*	30792	3.2	17	W	120	0.97 (58)	1.12	[0.31; 1.71]	69	$[25-1e4]$	61	1.6	3.1	.5
010612	9194	74.1	13	W	250	0.85 (89)	1.22	[1.07; 1.31]	592	$[274-1e4]$	462	7.2	49	.1
010613	27235	152.	38	W	250	1.32 (89)	1.40	[1.33; 1.47]	176	$[139-235]$	106	75	200	.3
010629	44468	15.1	28	W/I	200	0.92 (81)	1.17	[1.03; 1.31]	59	$[48-75]$	49	17	26	.6
010921	18950	24.6	44	W/I	200	1.23 (81)	1.49	[1.43; 1.56]	206	$[158-287]$	105	41	100	.4
010923	33870	3.8	60	I	250	1.06 (89)	1.74	[1.49; 2.04]	10000	$[347-1e4]$	2600	11	30	.3
010928	60826	48.3	24	W	400	0.95 (104)	.567	[.491; .639]	241	$[201-288]$	346	10	200	.0
011019	31370	25.4	25	W	80	0.76 (45)	1.75	[0.41; 2.47]	87	$[10-1e4]$	22	1.9	1.7	1.
011130	22775	83.2	26	W	70	0.97 (42)	1.08	$[-0.5; 2.51]$	32	$[16-1e4]$	29	0.9	0.7	1.
011212	14642	84.4	10	W	150	0.53 (67)	1.28	$[-3.0; 2.24]$	34	$[3-1e4]$	25	2.6	1.7	1.
011216	10524	31.8	47	I	100	1.33 (52)	1.82	[1.54; 2.11]	10000	$[420-1e4]$	1800	5.2	12.0	.4
020113[c]	7452	38.9	34	I	200	1.13 (81)	1.26	[0.74; 1.51]	511	$[79-1e4]$	378	2.2	13.2	.1
020124	38475	78.6	35	W	250	0.92 (89)	1.10	[0.98; 1.21]	133	$[101-186]$	120	18	68	.2
020127	75444	9.3	19	W	200	0.92 (81)	1.19	[1.00; 1.36]	156	$[97-330]$	126	2.4	9.1	.2
020201	65828	241.	53	W	80	0.95 (45)	1.67	[0.71; 2.16]	99	$[18-1e4]$	33	25	28	.9
020214[d]	67778	27.4	60	I	400	1.31 (104)	.256	[.059; .439]	176	$[145-219]$	307	32	930	.0
020305	42925	250.	36	W	250	1.16 (89)	.861	[.748; .968]	143	$[113-192]$	163	16	104	.1
020317	65731	3.3	23	W	150	1.08 (67)	1.01	$[-0.8; 1.95]$	44	$[11-1e4]$	44	1.2	1.7	.7
020331	59548	56.5	16	W	400	1.09 (104)	.922	[.812; 1.02]	120	$[97-153]$	129	9.0	45	.2

[a] This column indicates whether the burst has been localized by the WXM (W) or by the IPN (I).
[b] The fluences are in units of 10^{-7} erg cm^{-2} s^{-1}.
[c] GRB020113 is a probable short/hard burst, with $T_{50} = 0.6$ sec.
[d] The angle could be 54 or 64 degrees, a value of 60 degrees has been used here.

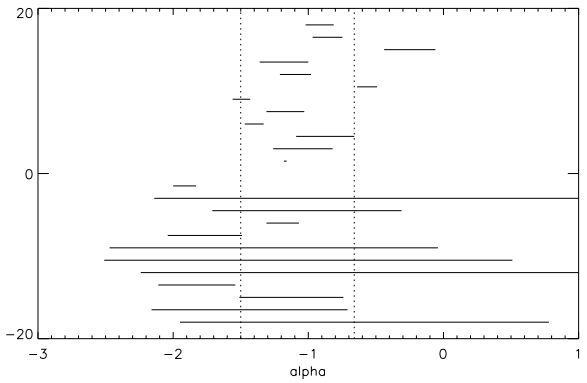

Fig. 4. Low energy spectral indices for 22 GRBs detected by FREGATE. The two vertical lines indicate the range of α expected for synchrotron radiation models. GRBs of group A(see text) have a positive ordinate.

ing at high energies (Lloyd & Petrosian 1999). Recently Heise et al. (2001) discovered short transients in the Wide Field Cameras of BeppoSAX, which had little or no emission in the GRBM, at energies above 40 keV. These events were called X-Ray Flashes (XRFs). Kippen et al. (2001) found 9 of these events in the untriggered BATSE data and performed a joint fit of the WFC+BATSE data in order to derive E_p for these XRFs. They find values ranging from 4 to 90 keV, much lower than the average for BATSE triggered GRBs.

The values of E_p computed for FREGATE GRBs are given in Table 1. It can be seen that E_p varies from 49 keV to 345 keV for the GRBs of group A, with only 1 event having E_p below 50 keV. In the absence of constraints on the values of E_0 for the GRBs of group B, it is difficult to derive reliable values for their E_p. Table 1 however shows that the GRBs of group B have higher values of L_x/L_γ, indicating softer spectra. Because the burst of group B are also significantly fainter, we discuss below whether the lack of statistics could influence their measured spectral properties. To this aim, we decreased the intensity of GRBs in the group A by a factor 6.5 to con-

struct a new set, A', with the same number of photons as group B GRBs, and computed the spectral parameters of this new set.

We characterize the spectral hardness of events in groups A, A' and B by two parameters: the average ratio L_x/L_γ and the fraction r of events with E_0 lower than 50 keV (even if E_0 is not well constrained for samples A' and B). We find that L_x/L_γ= 0.24±0.05, 0.27±0.07, and 0.81±0.14 for GRBs of group A, A' and B respectively, while r = 1/12, 1/12 and 7/12. These numbers show that the lower hardness of GRBs in group B is not an artefact resulting from their smaller number of photons. Since the high proportion of soft GRBs in group B cannot be due to their lower count rate, we are led to the conclusion that group B contains many intrinsically soft bursts which have too few photons around 100 keV to allow to constrain their E_0. This analysis also shows that the ratio L_x/L_γ is a robust estimator of the softness of our GRBs, and in the following we define soft GRBs as having L_x/L_γ greater than 0.60.

Based on this criterion we find that our sample contains 8 soft bursts from a total of 24 GRBs. While their E_p is not well defined, we consider that these 8 events certainly have E_p lower than 50 keV (which is the lower value of E_p measured in sample A). This percentage is comparable with 12 GRBs out of 22 with $E_p \leq$ 50 keV in the GINGA sample (Strohmayer et al. 1998) and with 17 out of 66 GRBs in the Bepposax/WFC sample (Heise et al. 2001). After GINGA and BeppoSAX, HETE-2 confirms the existence of a class of soft GRBs (with E_p lower than 50 keV). The connection of these soft GRBs with the population of "classical" GRBs with E_p of a few hundred keV is discussed in the next section.

3.2. XRFs and the Hardness-Intensity Correlation

Since FREGATE provides, for the first time, continuous coverage from 6 to 400 keV with a single instrument, it is ideally suited to study the question of whether events observed at low energies have the same properties as the classical GRBs observed at higher energies. In a first attempt to understand the possible connection between soft GRBs and classical GRBs, we use the fluence/fluence diagram plotted in Fig. 5. It is clear from this figure that there is no gap between the classical GRBs and the soft GRBs. Despite the small number of events, Fig. 5 rather suggests a continuous evolution of the GRB hardness with the intensity. This is the well known hardness-intensity correlation (hereafter HIC), but FREGATE shows that this correlation extends over 3 orders of magnitude in fluence. Another way to display the hardness-intensity correlation is given in Fig. 6 which shows the burst hardness (defined as the ratio of the fluence in the range 30-400 keV to the fluence in the range 6-30 keV) as a function of the total fluence.

In order to give a more quantitative statement on the significance of this correlation we computed the average hardness ratio for the brightest 12 GRBs and the faintest 12 GRBs in our sample. Taking into account only the statistical errors (which are dominant) we find $\log(L_x/L_\gamma)$ = -0.71 ± 0.12 for the bright GRBs and $\log(L_x/L_\gamma)$ = -0.22 ± 0.09 for the faint GRBs. While the difference is only significant at the 3.3 sigma level, we tend to believe it because it confirms the findings of other instruments (Atteia et al. 1994, Mallozzi et al. 1995, Dezalay et al. 1997, Atteia 2000). A linear fit of the correlation between the soft fluence (6-30 keV) and the hard fluence (30-400 keV) gives the following relation:

$F_{6-30} = 2\ 10^{-3} \times F_{30-400}^{0.608}$

In the past the origin of the hardness-intensity correlation in GRBs has been attributed to cosmological effects

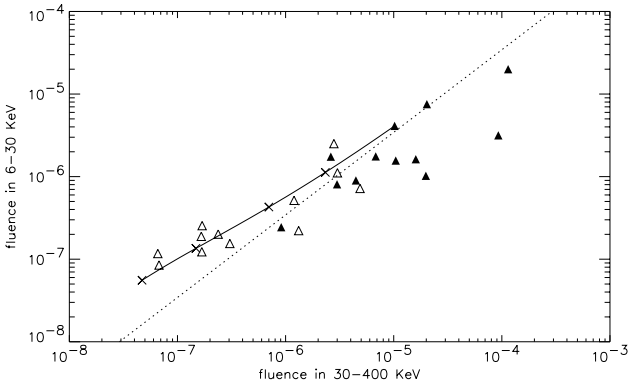

Fig. 5. Fluence in the energy range 6-30 keV as a function of the fluence in the range 30-400 keV. Dark triangles show group A GRBs (see text) and empty triangles group B bursts. The dotted line indicates events of constant hardness, the spectral hardness is higher below the line. The solid line shows how GRB010921 (at redshift z=0.45) would evolve on this plot if its redshift were increased from z=0.45 to z=10. the crosses indicate redshifts 1,2,5 and 10.

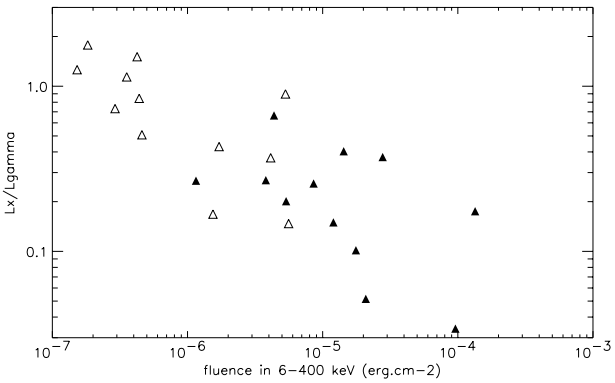

Fig. 6. Spectral hardness vs total fluence, showing the hardness-intensity correlation observed by FREGATE.

or to an intrinsic hardness-luminosity correlation. We discuss these two interpretations using the FREGATE data.

Fig. 5 plots the evolution of GRB010921 (Ricker et al. 2002) with the redshift (up to z=10) on a fluence/fluence diagram. The spectrum of GRB010921 was fit with a Band function with $\alpha = -1.42$, $\beta = -2.35$ and $E_0 = 170$ keV. For this study we used a Band function because it was not appropriate to neglect the high energy spectral index which plays an important role for GRBs at high redshift. We asssumed a flat universe with $\Omega_0 = 0.7$, $\Omega_\Lambda = 0.3$ and $H_0 = 65$ km sec^{-1} Mpc^{-1}. The figure shows that cosmological effects could in principle explain the observed correlation. In this case, however, we would also expect a significant time dilation of the soft GRBs.

Fig. 7 plots the duration T_{90} as a function of the total fluence. It shows that there is no significant time dilation of the faint GRBs. We should note here that because the widths of the peaks in the time histories of GRBs – and the durations of GRBs – are shorter at higher energies (e.g., Fenimore et al. 1995), this partly (but only partly) compensates for the time dilation due to the cosmological redshift. GRB durations go approximately like $E^{-0.4}$, so that this effect *shortens* the observed durations of GRBs at a redshift z = 10 relative to the durations of GRBs at a redshift z =1 by a factor of about $[(1+10)/(1+1)]^{0.4} = 2$. Time dilation would be expected to *increase* the duration of the bursts by $[(1+10)/(1+1)] = 5.5$. Thus, overall, one expects bursts at high redshifts to be longer by a factor of only about 2.7. Still, Fig. 7 does not support such a dependence.

While it is always possible to invoke GRB evolution to produce intrinsically shorter GRBs at high redhifts, we consider that our observations do not favor the interpretation of the HIC purely in terms of cosmological effects. Finally, we note that Amati et al. (2002) find a clear correlation between E_p and the radiated energy of 12 GRBs with known redshifts ($E_p = 100\ E_{52}^{0.52}$ keV, where E_{52} is the isotropic energy radiated in gamma-rays in units of 10^{52} ergs). This correlation, if it extends over a sufficient range of redshifts could certainly explain the hardness-intensity correlation we observe. With this interpretation, the HIC would be the reflection of a more fundamental correlation between the radiated energy and the spectral hardness in GRBs.

4. Conclusions

Our observations have two interesting consequences: they confirm that the E_p distribution is broader than previously thought (Mallozzi et al. 1995, Preece et al. 2000, Brainerd et al. 2000) and they show that we do not yet see the faint end of the GRB distribution. In fact if we assume that the correlation found by Amati et al. (2002) extends down to E_p as low as 20 keV, we must admit that the energy radiated by a GRB with $E_p = 20$ keV is about 80 times smaller that the energy radiated by a "typical" GRB with $E_p = 200$ keV.

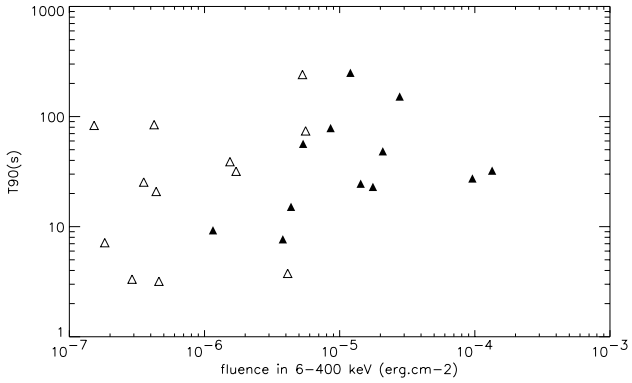

Fig. 7. GRB duration (T_{90}) as a function of the total fluence. This figure shows that faint GRBs are not significantly longer than bright events.

Future work with HETE will bring several advances in this field and should contribute to our understanding of the population of soft/faint GRBs. The continuously growing GRB sample of FREGATE should provide better statistical evidence for the effects discussed in this paper and additional clues about the possible differences between bright and faint GRBs. Joint spectral analysis with the WXM will allow more precise determinations of α and E_0 for soft GRBs. Finally, measuring the redshifts of a greater number of GRBs detected by HETE will allow us to test the extent of the correlation between the spectral hardness of GRBs and their radiated energy in gamma-rays. Soft GRBs also present an interesting challenge for future GRB missions, which will have to detect events which are much softer and fainter than the typical GRB population sampled by BATSE.

Acknowledgements. The HETE mission is supported in the US by NASA contract NASW-4690; in France by CNES contract 793-01-8479; and in Japan in part by the Minisitry of Education, Culture, Sports, Science and Technology Grant-in-Aid 13440063. KH is grateful for support under MIT contract SC-R-293291. The authors acknowledge the support of the HETE operation team.

References

Amati, L. et al. 2002, submitted to A&A
Atteia, J.-L. et al. 1994, A&A, 288, 213
Atteia, J.-L. 2000, A&A, 353, L18
Atteia, J-L. et al. 2002, AIP Conference Proceedings, ???, ???.
Band, D. et al. 1993, ApJ, 413, 281.
Brainerd, J. J., Pendleton, G. N., Mallozzi, R. S., Briggs, M. S., & Preece, R. D. 2000, AIP Conf. Proc. 526: Gamma-ray Bursts, 5th Huntsville Symposium, 150
Brainerd, J. et al. 2001, Manuscript available on request from the author
Cohen, E., Katz, J. I., Piran, T., Sari, R., Preece, R. D., & Band, D. L. 1997, ApJ, 488, 330
Daigne, F. & Mochkovitch, R. 1998, MNRAS, 296, 275

Dezalay, J.-P. et al. 1997, ApJ, 490, L17
Fenimore, E. E., in 't Zand, J. J. M., Norris, J. P., Bonnell, J. T., & Nemiroff, R. J. 1995, ApJ, 448, L101
Frontera, F. et al. 2000, ApJS, 127, 59.
Heise, J., in't Zand, J., Kippen, R. M., & Woods, P. M. 2001, Gamma-Ray Bursts in the Afterglow Era, Proceedings of the International workshop held in Rome, CNR headquarters, 17-20 October, 2000. Edited by Enrico Costa, Filippo Frontera, and Jens Hjorth. Berlin Heidelberg: Springer, 2001, p. 16., 16.
Kawai, N. et al. 2002, AIP Conference Proceedings, ???, ???.
Kippen, R. M., Woods, P. M., Heise, J., in't Zand, J., Preece, R. D., & Briggs, M. S. 2001, Gamma-Ray Bursts in the Afterglow Era, Proceedings of the International workshop held in Rome, CNR headquarters, 17-20 October, 2000. Edited by Enrico Costa, Filippo Frontera, and Jens Hjorth. Berlin Heidelberg: Springer, 2001, p. 22., 22.
Lamb, D. Q. et al. 2002, ApJ, submitted.
Lloyd, N. M. & Petrosian, V. ; 1999, ApJ, 511, 550.
Lloyd, N. M. & Petrosian, V. ; 2000, ApJ, 543, 722
Lloyd N. 2002, AIP Conference Proceedings, ???, ???.
Mallozzi, R. S., Paciesas, W. S., Pendleton, G. N., Briggs, M. S., Preece, R. D., Meegan, C. A., & Fishman, G. J. 1995, ApJ, 454, 597.
Mészáros, P. & Rees, M. J. 2000, ApJ, 530, 292
Olive, J-F. et al. 2002, AIP Conference Proceedings, ???, ???.
Panaitescu, A. & Meszaros, P. 1998, ApJ, 501, 772
Panaitescu, A. & Mészáros, P. 2000, ApJ, 544, L17
Piran, T. 2000, Phys. Rep., 333, 529
Preece, R. D., Briggs, M. S., Mallozzi, R. S., Pendleton, G. N., Paciesas, W. S., & Band, D. L. 1998, ApJ, 506, L23.
Preece, R. D., Briggs, M. S., Mallozzi, R. S., Pendleton, G. N., Paciesas, W. S., & Band, D. L. 2000, ApJS, 126, 19
Rees, M. J. & Meszaros, P. 1994, ApJ, 430, L93
Ricker, G. R. et al. 2002, ApJ, accepted.
Sari, R., Narayan, R., & Piran, T. 1996, ApJ, 473, 204
Sari, R. & Piran, T. 1997, MNRAS, 287, 110
Sari, R. & Mészáros, P. 2000, ApJ, 535, L33
Strohmayer, T. E., Fenimore, E. E., Murakami, T., & Yoshida, A. 1998, ApJ, 500, 873.
Villasenor, J.S. et al. 2002, AIP Conference Proceedings, ???, ???.
Zhang B. & Mészáros, P. 2000, astro-ph/0206158